

Revisiting the Stöber Method: Inhomogeneity in Silica Shells

Yi Jian Wong,[†] Liangfang Zhu,[†] Wei Shan Teo,[†] Yan Wen Tan,[†] Yanhui Yang,[#] Chuan Wang,^{*,†} and Hongyu Chen^{*,†}

[†]Division of Chemistry and Biological Chemistry, Nanyang Technological University, Singapore 637371

[#]Institute of Chemical Engineering and Sciences, 1 Pesek Road, Jurong Island, Singapore 627833

^{*}Division of Chemical and Biomolecular Engineering, Nanyang Technological University, Singapore 637459

S Supporting Information

ABSTRACT: We demonstrate that the silica shell on nanoparticles formed by a typical Stöber method is inhomogeneous in nature. The outer layer of the shell is chemically more robust than the inner layer, which can be selectively etched by hot water. Methods are developed to “harden” the soft silica shells. These new understandings are exploited to develop versatile and template-free approaches for fabricating sophisticated yolk–shell nanostructures.

Core–shell nanostructure is a popular structural scheme for enhancing the chemical and colloidal stability of nanoparticles (NPs) and for preventing the dissociation of their surface ligands.¹ In particular, silica has advantages as a shell material for its chemical inertness, optical transparency, porous structure, and size-selective permeability.² The Stöber method has attracted much interest for the scalable fabrication of silica shells on NPs via the facile hydrolysis of tetraethyl orthosilicate (TEOS).³ While the direct analysis of the resulting nanoscale silica shells is difficult, it is generally believed that the complete hydrolysis of TEOS and the subsequent condensation of silicic acid give a network of tetrahedral SiO₄ units with shared vertices. As such, the silica shells are expected to be uniform and robust, though their uniformity has rarely been explored.

Recently, the advance of synthetic control has led to more complex core–shell nanostructures, including multilayer NPs.⁴ In particular, the so-called “yolk–shell” NPs containing a void space between a core and the outer shell have received much attention.^{2b–d,5} An enclosed void space is perceived to be useful for chemical storage and compartmentation in applications such as catalysis,^{2b,c,6} drug delivery,⁷ and energy storage.⁸ Most importantly, the space in the yolk–shell nanostructure provides a unique environment for creating potentially concerted actions between the core and a permeable barrier. Thus, shells with controllable permeability such as silica shells are particularly sought after.

Most of the yolk–shell NPs in the literature were fabricated by removing the intermediate layer in multilayer NPs.⁹ The process was synthetically challenging, since multistep depositions were often necessary for preparing multilayer NPs, and subsequently, the intermediate layer has to be selectively removed. The structural parameters of the yolk–shell NPs were directly obtained from those of the multilayer NPs, and thus, they were dependent on the consistency and reproducibility of the prior steps.

There have been several advances in the facile fabrication of silica-based yolk–shell NPs. Yin and co-workers reported the direct fabrication of yolk–shell NPs by simultaneous dissolution

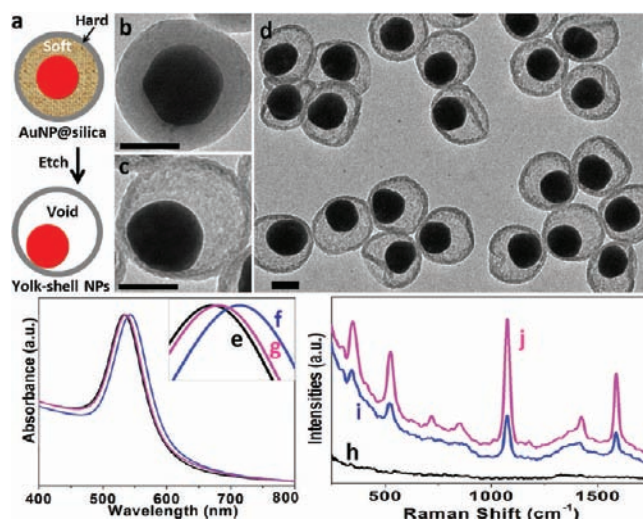


Figure 1. (a) Schematics illustrating the formation of yolk–shell NPs. TEM images of (b) AuNP@silica and (c,d) yolk–shell NPs at high and low magnification, respectively. Normalized UV–vis spectra of (e) AuNPs, (f) AuNP@silica, and (g) yolk–shell NPs. Raman spectra of (h) AuNPs, (i) (AuNP-MBA)@silica, and (j) the yolk–shell NPs derived from (AuNP-MBA)@silica. Scale bars = 50 nm. See large-area views in S1.

and deposition of silica.^{5b} Haes and co-workers reported one-pot sequential hydrolysis of 3-aminopropyltriethoxysilane (APTES) and TEOS to give a proposed double-layered shell.¹⁰ The APTES-derived layer was selectively dissolved in NH₃·H₂O to give yolk–shell NPs. In a different approach, Yin's group used only TEOS to generate core–shell NPs. They showed that polyvinylpyrrolidone (PVP) can protect the outmost silica layer to allow selective etching of the inner section.¹¹ Two recent reports revealed that the inner silica section can also be selectively etched in the absence of PVP^{11b} or other protective agents,^{12a} but the origin of this selectivity remained illusive. Since the silica shells arising from the Stöber method are perceived to be homogeneous in nature, engineering them with different composition or stability becomes critically important for selective etching.

Here, we give unambiguous evidence that the silica shells from a typical Stöber method are inhomogeneous. As such, we can choose conditions to directly and selectively etch the inner shell section to achieve a yolk–shell motif (Figure 1). While direct

Received: April 11, 2011

Published: July 06, 2011

analysis of the shell composition remains challenging, we resort to detailed reactions to probe the origin of the inhomogeneity. With this new understanding, yolk–shell NPs can be fabricated by facile and reproducible syntheses and their structural parameters readily tailored. For example, “nano-matryoshkas” only 250 nm in diameter are synthesized with four yolk–shell motives. The synthesis compares favorably to traditional approaches that would have required eight-layered NPs before etching.

We used a typical Stöber method as follows: As-synthesized citrate-stabilized AuNPs ($d = 62$ nm) were centrifuged to remove sodium citrate and the aqueous supernatant, before they were added to 11-mercaptoundecanoic acid (MUA) in 2-propanol. The solution was stirred vigorously for 10 min, before TEOS and ammonia were added.¹³ The final mixture (2-propanol/water = 2:1, v/v) was incubated at room temperature (RT) overnight (10–14 h). The resulting core-shell NPs (AuNP@silica) were isolated by centrifugation, redispersed in ethanol, and then characterized by transmission electron microscopy (TEM, Figure 1b).¹³

To our surprise, the purified AuNP@silica can be directly turned to yolk–shell NPs (Figure 1c,d) simply by incubating in water at 90 °C for 30 min. It was clear that the inner section of the silica shell was etched away, leading to a reduced TEM contrast in the intermediate layer. In most cases, the AuNPs were displaced from their original central position as the resulting void gave them freedom. Some of the shells appeared collapsed in Figure 1d, but for the intact ones, the overall diameter (108 ± 8 nm) was barely changed from those before the etching (113 ± 6 nm). On the basis of this observation, we believe that the outmost layer of the original silica shells persisted.

After the silica encapsulation, the AuNP plasmon absorption peak shifted from 533 to 543 nm (Figure 1e–f), indicating an increase in the refractive index near Au.¹⁴ The absence of an absorption peak at 600–800 nm suggested that the AuNPs were not aggregated.¹⁵ After etching, as the silica near the Au surface was replaced by water, the AuNP absorption (536 nm, Figure 1g) nearly returned to the original peak position of citrate-stabilized AuNPs. It is known in the literature that ligands with terminal carboxylic acid, such as MUA, can render a Au surface amenable for silica adsorption.^{1c,16} Thus, MUA can be replaced by similar ligands such as the SERS-active 4-mercaptobenzoic acid (MBA).^{16a} The (MBA-AuNP)@silica can be etched in a way similar to the etching of NPs functionalized with MUA. Observation of the MBA signal¹⁷ before and after the etching (Figure 1i,j) confirmed the location of the ligands on the Au surface.

The silica shells must be porous and permeable to allow the solvent to diffuse in and the shell to dissolve out. However, the fact that the inner silica layer was preferentially dissolved was intriguing: the rates of materials transport must be a factor for the etching, but the inner layer was obviously less exposed to the solvent than the outer layer. Previously, silica shells were unevenly etched using two types of silica precursors¹⁰ or using PVP as a protecting agent.^{11a–d} In our system, the reaction mixture contained only TEOS, ammonia, MUA, citrate, and AuNPs. In control experiments, silica spheres synthesized in the absence of MUA, citrate, and AuNPs were able to form hollow structures^{12a} under similar etching conditions (Figure 2b,c), indicating that those three ingredients were not the cause of the selective etching. 2-Propanol can be replaced by ethanol in preparing AuNP@silica that can be similarly etched to give yolk–shell NPs. If ammonia were responsible, its effect should have been uniform throughout the shells. Thus, there is no likely candidate as the protecting agent. We postulated that the silica shells must be inhomogeneous in nature, which seems to be reasonable considering the sequential hydrolysis of TEOS in water.

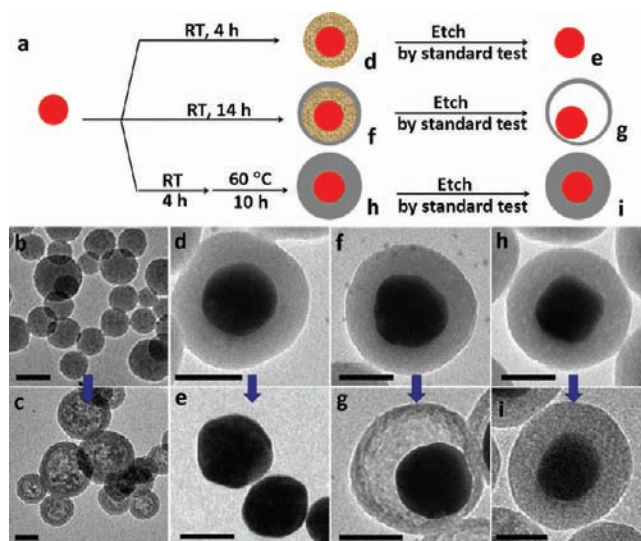


Figure 2. (a) Schematic illustrations and (b–i) TEM images showing the experimental conditions and typical nanostructures before (b,d,f,h) and after (c,e,g,i) the standard etching tests: (b,c) silica NPs, 14 h at RT; (d,e) AuNP@silica, 4 h at RT; (f,g) AuNP@silica, 14 h at RT; (h,i) AuNP@silica, 4 h at RT and 10 h at 60 °C. Scale bars = 50 nm.

From the TEM images, the silica shell of AuNP@silica appeared to be homogeneous, but chemically it was not. Hence, we must probe the nature of the shells in a series of reactions. On the basis of the hypothesis above, one would expect the continuous hydrolysis of TEOS to give a smooth gradient in terms of chemical stability in the shell. Indeed, hot water etched the silica shells in a progressive manner; over a prolonged period of time (>1 h), even the harder outmost silica layer in Figure 1d started to disintegrate. For the convenience of discussion, we arbitrarily define the silica shells as follows: We define a “standard test”, whereby the isolated AuNP@silica was incubated in water at 90 °C for 30 min. The etchable section under the standard test is defined as “soft”, whereas the remaining section is defined as “hard”. In Figure 1d, the hard section was estimated to be about 9.9 ± 0.5 nm thick.

Our first realization was that the stability of the shells depended on the conditions under which they were formed. The AuNP@silica that underwent 4 h incubation at RT in the preparative solution was completely etched in the standard test (Figure 2d,e), in contrast to the NPs that underwent 14 h incubation and gave the yolk–shell NPs (Figure 2f,g). It appears that the species in the preparative solution led to the selective hardening of the outer layer, possibly by additional silica deposition or further cross-linking of the silica matrix. We searched for a hardening recipe to gain insight in this chemistry and found that incubation of the AuNP@silica in the preparative solution at elevated temperature (60 °C) could render the inner soft section unetchable in the standard test (Figure 2h,i). Such hardened AuNP@silica can still be partially etched under harsher conditions (e.g., at 100 °C in water for 17 h).¹³ Control experiments established that TEOS or its derivatives were the critical factor in the hardening chemistry: the soft AuNP@silica isolated after 4 h was incubated with only TEOS in 2-propanol/water (v/v = 2:1) for 10 h at 60 °C. The entire silica shell was hardened.¹³

Further experiments were carried out to narrow down the key conditions for the selective hardening. The soft AuNP@silica was isolated after 4 h incubation at RT (same as Figure 2d); the sample was repeatedly centrifuged and redispersed in 2-propanol, so that any excess chemical in the solution was removed. To our surprise,

however, when this purified sample of AuNP@silica was heated in neat 2-propanol at 60 °C for 10 h (Figure 3b), the outer layer of the shells was hardened: after the standard test, yolk–shell NPs resulted (Figure 3c). Control experiments confirmed that heating by itself did not have the hardening effect: a sample of the same purified AuNP@silica was incubated in water at 60 °C for 10 h, and its shell was completely removed (Figure 3a). Since all solution chemicals have been removed, the hardening of the outer section shown in Figure 3b,c clearly was due not to the additional deposition of substances but to the chemical transformation (e.g., cross-linking) *within* the shell. Most likely, there were preexisting differences in the chemical composition of the different sections of the silica shell.

However, there is an alternative explanation: the selective hardening of the outer layer could be due either to its reaction with the solution species or to the surface recondensation of the dissolved silica. To investigate this possibility, we prepared AuNP@silica using three cycles of silica deposition at RT for 4 h each, with proper isolation and purification steps in between.¹³ Subsequently, the purified AuNP@silica was incubated in neat 2-propanol at 60 °C for 72 h to ensure the hardening of all three layers (Figure 3d). After the standard etching test, multilayered yolk–shell motives can be discerned in the resulting matryoshka-like nanostructures (Figure 3e). Thus, the above arguments of protecting agent (e.g., residue ammonia) or silica recondensation cannot explain the hardening of the inner sections, particularly the uniform thickness of all hardened layers. This result was an unambiguous indication that the chemical compositions of hard and soft sections were different even *before* the hardening process.

There is an interesting contrast between panels a and b of Figure 3: with all other conditions unchanged, heating in 2-propanol hardened the shell, whereas doing so in water etched it. It is clear that water played an important role in etching the silica shell;^{12b} the use of 2-propanol removed water and thus enabled the hardening of the shell (e.g., by cross-linking). Control experiments showed that heating in neat DMF had a similar hardening effect.¹³ Hence, the two organic solvents probably played a passive role: it is unlikely that they could both be involved in the same hardening chemistry.

While further studies are imperative to understand the molecular details of the silica shells, the following hypothesis serves well as a working model that is so far consistent with all of our results. TEOS undergoes consecutive hydrolysis in water to give 1–4 hydroxyl groups.¹⁸ The simultaneous condensation of these species makes it difficult to examine the reactive intermediates. Given the slow TEOS hydrolysis, a gradient of increasing chemical stability forms as the TEOS derivatives deposited on the Au surface are increasingly hydrolyzed. As such, the outermost layer is “hardest” (Figure 2f,g), as it is mostly derived from the condensation of silicic acid and its aggregates. In comparison, the innermost layer is “softest”, with a porous structure, which could result from a lower degree of cross-linking and/or a higher degree of swelling (more solvent was present owing to more ethoxy groups therein). Such porosity could explain the hardening of the softest layer upon heating in the preparative solution (Figure 2h,i) and its inability to be hardened when heated alone in neat 2-propanol (Figure 3d,e). Obviously, TEOS or its derivatives played a critical role in bridging and cross-linking the porous section. In the sample that underwent 4 h incubation at RT, the outermost layer has intermediate “hardness”, as it is soft but has enough density to be cross-linked when heated in neat 2-propanol.

With our new understanding of the selective etching and hardening conditions, new methods for synthetic control of yolk–shell NPs can be developed. A variety of yolk–shell

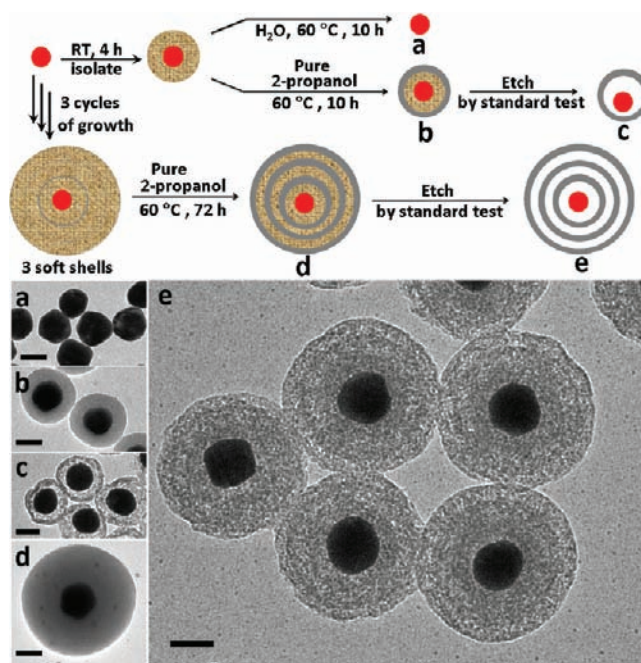


Figure 3. Schematic illustrations and TEM images for analyzing the hardening chemistry. AuNP@silica (4 h at RT) was isolated and either (a) incubated in water at 60 °C for 10 h or (b) first incubated in neat 2-propanol at 60 °C for 10 h, and then (c) etched by the standard test. In a different set of reactions, AuNP@silica was coated with three layers of soft shell, isolated, (d) hardened in neat 2-propanol at 60 °C for 72 h, and then (e) etched by the standard test. Scale bars = 50 nm.

nanostructures can be obtained using different combinations of the following processes: (a) soft silica shell can be prepared using 2 h incubation at RT in the preparative solution to ensure its “softness”; (b) partially hardened shell (denoted as h/s) can be prepared by 10–14 h incubation at RT; and (c) hard shell can be prepared using 10 h incubation at 60 °C. In addition, postsynthesis hardening of the soft section is also possible, as discussed above.

The void space in the yolk–shell NPs can be readily tuned (Figure 4). Citrate-AuNPs were coated with one h/s layer; after etching, yolk–shell NPs were obtained with a boundary of ~100 nm (Figure 4a,b). In comparison, the yolk–shell NPs obtained from three soft layers and one h/s layer have a boundary of ~200 nm (Figure 4d, e). Obviously, the void space in the NPs of Figure 4e was much larger than that of the NPs of Figure 4b. Both types of yolk–shell NPs appeared collapsed under TEM. The etched NPs (Figure 4b,e) were isolated and coated with an additional silica layer to preserve the shell conformation as it was in solution. As shown in the resulting TEM images (Figure 4c,f), none of the yolk–shell NPs collapsed, suggesting that the previous collapsing did not occur in solution, but was a result of the drying process of TEM sample preparation.

The nano-matryoshkas¹⁹ in Figure 3e did not show clear boundaries, and thus we attempted an improved synthesis (Figure 4g,h): Citrate-AuNPs were coated with four h/s layers in four consecutive steps. The isolated product was then etched in one step in hot water.¹³ As shown in Figure 4h, the void/shell contrast in the resulting matryoshka-like nanostructure was much better than that of the NPs in Figure 3e. In general, we found that the hardened layers created in the preparative solution were better than those created by heating isolated NPs in 2-propanol. The nano-matryoshkas showed four layers of yolk–shell motives but have diameters of only 250 nm.

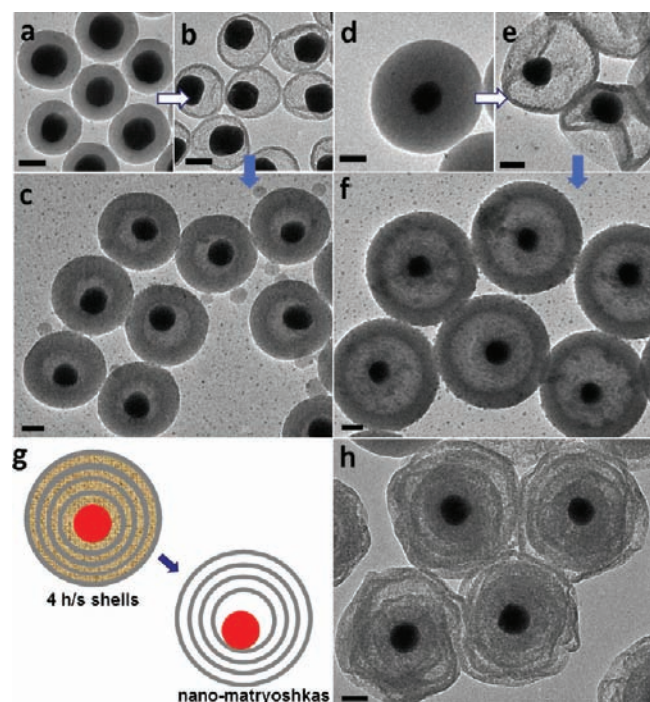


Figure 4. Strategy to modulate the void space in yolk–shell NPs. TEM images of (a) AuNP@silica with one h/s silica shell and yolk–shell NPs with small void space (b) before and (c) after coating of an additional shell. (d–f) TEM images of similar nanostructures derived from AuNP@silica with three soft spacer shells. (g,h) Schematics and TEM images of nano-matryoshkas. Scale bars = 50 nm.

In comparison to traditional methods, the simultaneous fabrication of hard and soft spacer layers leads to easier synthesis, making multiple yolk–shell motives readily accessible. Moreover, our colloidal method does not require high-temperature calcination,^{5d,11e} which could induce NP aggregation and limit the scalability of the synthesis.

In summary, we have provided unambiguous evidence for the inhomogeneity in the silica shells. The Stöber method is widely used for passivating various nanoparticles in many applications, where understanding the chemical stability of the resulting shell is of critical importance. In particular, awareness of the inhomogeneity will improve the control of permeability and the interpretation of the loading capacity of silica-based nanoparticles. In this report, we provide specific conditions to etch or harden the silica shells, and we further demonstrate that the inhomogeneity can be exploited for novel synthetic control of silica nanostructures.

■ ASSOCIATED CONTENT

S Supporting Information. Details of procedures, methods, and large-area views of TEM images. This material is available free of charge via the Internet at <http://pubs.acs.org>.

■ AUTHOR INFORMATION

Corresponding Author

hongyuchen@ntu.edu.sg; wang_chuan@ices.a-star.edu.sg

■ ACKNOWLEDGMENT

The authors thank MOE (ARC 13/09) and A*STAR (102-152-0018) of Singapore for financial supports.

■ REFERENCES

- (1) (a) Scharrtl, W. *Nanoscale* **2010**, *2*, 829. (b) Guerrero-Martínez, A.; Pérez-Juste, J.; Liz-Marzán, L. M. *Adv. Mater.* **2010**, *22*, 1182. (c) Wallace, A. F.; DeYoreo, J. J.; Dove, P. M. *J. Am. Chem. Soc.* **2009**, *131*, 5244. (d) Chen, G.; Wang, Y.; Yang, M.; Xu, J.; Goh, S. J.; Pan, M.; Chen, H. *J. Am. Chem. Soc.* **2010**, *132*, 3644. (e) Yang, M.; Chen, T.; Lau, W. S.; Wang, Y.; Tang, Q.; Yang, Y.; Chen, H. *Small* **2009**, *5*, 198.
- (2) (a) Mulvaney, S. P.; Musick, M. D.; Keating, C. D.; Natan, M. J. *Langmuir* **2003**, *19*, 4784. (b) Lee, J.; Park, J. C.; Bang, J. U.; Song, H. *Chem. Mater.* **2008**, *20*, 5839. (c) Lee, J.; Park, J. C.; Song, H. *Adv. Mater.* **2008**, *20*, 1523. (d) Deng, Y.; Deng, C.; Qi, D.; Liu, C.; Liu, J.; Zhang, X.; Zhao, D. *Adv. Mater.* **2009**, *21*, 1377. (e) Lai, X.; Li, J.; Korgel, B. A.; Dong, Z.; Li, Z.; Su, F.; Du, J.; Wang, D. *Angew. Chem., Int. Ed.* **2011**, *50*, 2738.
- (3) Stöber, W.; Fink, A.; Bohn, E. *J. Colloid Interface Sci.* **1968**, *26*, 62.
- (4) (a) Pan, M.; Xing, S.; Sun, T.; Zhou, W.; Sindoro, M.; Teo, H. H.; Yan, Q.; Chen, H. *Chem. Commun.* **2010**, 46, 7112. (b) Xing, S.; Feng, Y.; Tay, Y. Y.; Chen, T.; Xu, J.; Pan, M.; He, J.; Hng, H. H.; Yan, Q.; Chen, H. *J. Am. Chem. Soc.* **2010**, *132*, 9537. (c) Lou, X. W.; Yuan, C.; Archer, L. A. *Small* **2007**, *3*, 261.
- (5) (a) Kamata, K.; Lu, Y.; Xia, Y. *J. Am. Chem. Soc.* **2003**, *125*, 2384. (b) Zhang, T.; Ge, J.; Hu, Y.; Zhang, Q.; Aloni, S.; Yin, Y. *Angew. Chem., Int. Ed.* **2008**, *47*, 5806. (c) Liu, J.; Qiao, S. Z.; Budi Hartono, S.; Lu, G. Q. *Angew. Chem., Int. Ed.* **2010**, *49*, 4981. (d) Liu, J.; Hartono, S. B.; Jin, Y. G.; Li, Z.; Lu, G. Q.; Qiao, S. Z. *J. Mater. Chem.* **2010**, *20*, 4595.
- (6) Huang, X.; Guo, C.; Zuo, J.; Zheng, N.; Stucky, G. D. *Small* **2009**, *5*, 361.
- (7) (a) Li, L.; Tang, F.; Liu, H.; Liu, T.; Hao, N.; Chen, D.; Teng, X.; He, J. *ACS Nano* **2010**, *4*, 6874. (b) Wang, T.; Chai, F.; Fu, Q.; Zhang, L.; Liu, H.; Li, L.; Liao, Y.; Su, Z.; Wang, C.; Duan, B.; Ren, D. *J. Mater. Chem.* **2011**, *21*, 5299. (c) Tang, S.; Huang, X.; Chen, X.; Zheng, N. *Adv. Funct. Mater.* **2010**, *20*, 2442.
- (8) (a) Liu, J.; Xia, H.; Xue, D.; Lu, L. *J. Am. Chem. Soc.* **2009**, *131*, 12086. (b) Lee, K. T.; Jung, Y. S.; Oh, S. M. *J. Am. Chem. Soc.* **2003**, *125*, 5652.
- (9) (a) Xing, S.; Tan, L. H.; Chen, T.; Yang, Y.; Chen, H. *Chem. Commun.* **2009**, 1653. (b) Zhu, J.; Sun, T.; Hng, H. H.; Ma, J.; Boey, F. Y. C.; Lou, X.; Zhang, H.; Xue, C.; Chen, H.; Yan, Q. *Chem. Mater.* **2009**, *21*, 3848. (c) Li, J.; Zeng, H. C. *Angew. Chem., Int. Ed.* **2005**, *44*, 4342.
- (10) Roca, M.; Haes, A. J. *J. Am. Chem. Soc.* **2008**, *130*, 14273.
- (11) (a) Zhang, Q.; Ge, J.; Goebel, J.; Hu, Y.; Lu, Z.; Yin, Y. *Nano Res.* **2009**, *2*, 583. (b) Hu, Y.; Zhang, Q.; Goebel, J.; Zhang, T.; Yin, Y. *Phys. Chem. Chem. Phys.* **2010**, *12*, 11836. (c) Zhang, Q.; Zhang, T.; Ge, J.; Yin, Y. *Nano Lett.* **2008**, *8*, 2867. (d) Zhang, Q.; Lee, I.; Ge, J.; Zaera, F.; Yin, Y. *Adv. Funct. Mater.* **2010**, *20*, 2201. (e) Huang, C. C.; Huang, W.; Yeh, C. S. *Biomaterials* **2011**, *32*, 556.
- (12) (a) Park, S.-J.; Kim, Y.-J.; Park, S.-J. *Langmuir* **2008**, *24*, 12134. (b) Yu, Q.; Wang, P.; Hu, S.; Hui, J.; Zhuang, J.; Wang, X. *Langmuir* **2011**, *27*, 7185.
- (13) See Supporting Information for large-area images and details.
- (14) Chen, H. Y.; Abraham, S.; Mendenhall, J.; Delamarre, S. C.; Smith, K.; Kim, I.; Batt, C. A. *ChemPhysChem* **2008**, *9*, 388.
- (15) Yang, M.; Chen, G.; Zhao, Y.; Silber, G.; Wang, Y.; Xing, S.; Han, Y.; Chen, H. *Phys. Chem. Chem. Phys.* **2010**, *12*, 11850.
- (16) (a) Chen, T.; Chen, G.; Xing, S.; Wu, T.; Chen, H. *Chem. Mater.* **2010**, *22*, 3826. (b) Xue, C.; Chen, X.; Hurst, S. J.; Mirkin, C. A. *Adv. Mater.* **2007**, *19*, 4071. (c) Liz-Marzán, L. M.; Giersig, M.; Mulvaney, P. *Chem. Commun.* **1996**, 731. (d) Liz-Marzán, L. M.; Giersig, M.; Mulvaney, P. *Langmuir* **1996**, *12*, 4329.
- (17) Chen, T.; Wang, H.; Chen, G.; Wang, Y.; Feng, Y.; Teo, W. S.; Wu, T.; Chen, H. *ACS Nano* **2010**, *4*, 3087.
- (18) (a) van Blaaderen, A.; Kentgens, A. P. M. *J. Non-Cryst. Solids* **1992**, *149*, 161. (b) van Blaaderen, A.; Van Geest, J.; Vrij, A. *J. Colloid Interface Sci.* **1992**, *154*, 481.
- (19) (a) Prodan, E.; Radloff, C.; Halas, N. J.; Nordlander, P. *Science* **2003**, *302*, 419. (b) Chung, H. Y.; Guo, G. Y.; Chiang, H.-P.; Tsai, D. P.; Leung, P. T. *Phys. Rev. B* **2010**, 165440.